Seasonal variability of the Black Sea chlorophyll-*a* concentration

Peter C. Chu[a,*], Leonid M. Ivanov[b], Tatyana M. Margolina[b]

[a]*Naval Ocean Analysis and Prediction Laboratory, Department of Oceanography, Naval Postgraduate School, Monterey CA, 93943 USA*
[b]*Marine Hydrophysical Institute, Ukrainian National Academy of Sciences, Ukraine*

Abstract

The optimal spectral decomposition (OSD) method is used to reconstruct seasonal variability of the Black Sea horizontally averaged chlorophyll-*a* concentration from data collected during the NATO SfP-971818 Black Sea Project in 1980–1995. During the reconstruction, quality control is conducted to reduce errors caused by measurement accuracy, sampling strategy, and irregular data distribution in space and time. A bi-modal structure with winter/spring (February–March) and fall (September–October) blooms is uniquely detected and accurately documented. The chlorophyll-*a* enriched zone rises to 15 m depth in winter and June, and deepens to 40 m in April and 35 m in August. The June rise of the chlorophyll-*a* enriched zone is accompanying by near-continuous reduction of upper layer maximum chlorophyll-*a* concentration.
© 2005 Elsevier B.V. All rights reserved.

1. Introduction

Observational (in-situ and remote sensing) and modeling studies show rapid change and deterioration of the Black Sea ecosystem. The abruptly increased nutrients and contaminants, that are delivered to the northwest shelf zone with river runoffs and redistributed within the entire water body, have induced a severe basin-scale eutrophication of the Black Sea water (Mee, 1992; Zaitsev and Mamaev, 1997; Yilmaz et al., 2001; Oguz et al., 2002a).

The chlorophyll-*a* concentration is considered to be the main measure of phytoplankton biomass and has been intensively discussed as applied to the Black Sea in a variety of aspects including patterns of spatial distribution, seasonal and inter-annual variability (Vedernikov and Demidov, 1993, 1997; Oguz et al., 2002b; Kopelevich et al., 2002; Yunev et al., 2002; Moncheva, 2003).

The chlorophyll-*a* data come from two major sources: in-situ measurements and satellite (CZCS and SeaWiFS) images. The in-situ data are noisy (noise-to-signal ratio up to 60%), sparse and irregular in space and time (Vedernikov and Demidov, 1997). The satellite data (SeaWiFS images) are also noisy

---

* Corresponding author.
  E-mail address: chu@nps.navy.mil (P.C. Chu).

with the noise-to-signal ratio near 35% for open water and higher for turbid coastal water such as the Black Sea (Srokosz, 2000; Oguz et al., 2002b).

Different types of seasonal variability of the basin-scale Black Sea chlorophyll-*a* concentration have been identified using the two kinds of data sources and traditional statistical methods. A bi-modal structure with winter/spring and fall blooms is considered to exist in the phytoplankton annual cycle in the middle latitudes (Longhurst, 1995; Sathyendranath et al., 1995) and must appear in the Black Sea as well. The February–March bloom presents a pronounced signal in the chlorophyll-*a* measurements, and so it has been clearly detected using both in-situ and satellite data (Vedernikov and Demidov, 1997; Oguz et al., 2002b, 2003, among others). It is not the case for the fall bloom, the existence of which was surmised from the satellite data analysis (Oguz et al., 2002b, 2003), but was not evidently proved through the in-situ measurements (Vedernikov and Demidov, 1997; Yunev et al., 2002).

A question arises: How many blooms are there in the seasonal variability of the Black Sea chlorophyll-*a* concentration? Since the satellite data are more regularly sampled in space and time than the in-situ data, a reasonable guess may favor the two blooms, but ultimate confirmation of the two-bloom structure still needs the in-situ data with its vertical sampling (subsurface information). Since the in-situ data are highly noisy and irregularly sampled, the traditional statistical methods might not be sufficient. Methods with the capacity to process noisy and sparse data should be used.

Recently, an optimal spectral decomposition (OSD) method was developed to reconstruct noisy and sparse scalar fields as well as Eulerian and Lagrangian velocity data. This method is robust to various noise-to-signal ratios, number of observations, and sampling strategy (Chu, 1999; Chu et al., 2003a,b). For example, reliable data sets were obtained for radionuclide pollution of the Black, White, and Kara Seas using the OSD method
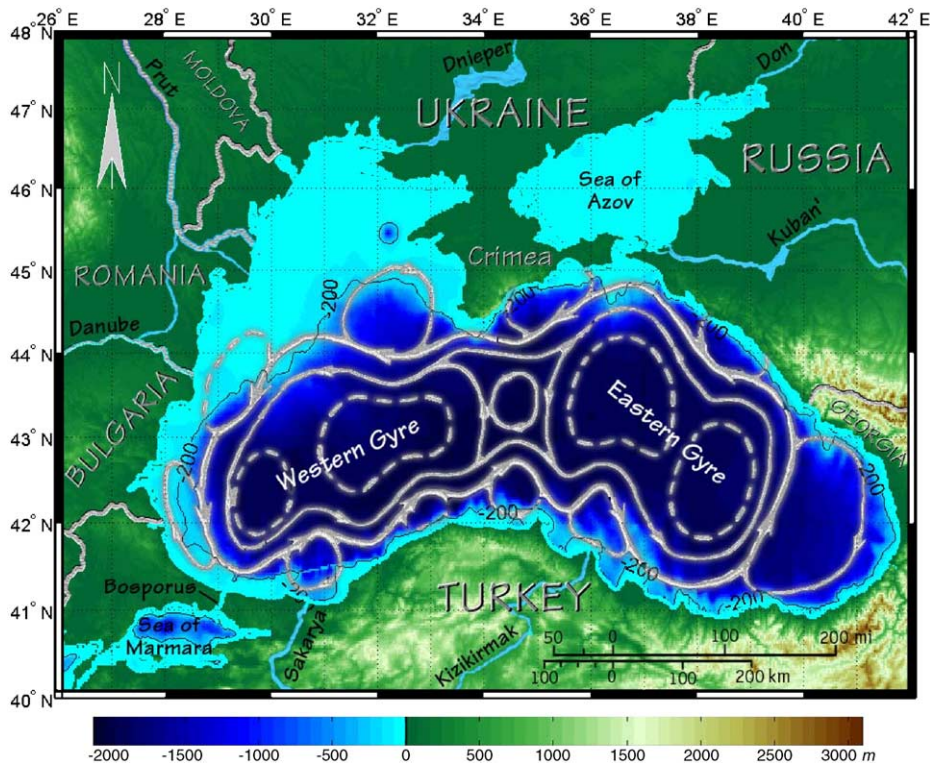

Fig. 1. The Black Sea geography, bottom topography, and circulations (Oguz et al., 1993).

(Ivanov et al., 2001, 2004; Eremeev et al., 1994, 1995; Danilov et al., 1996; Ivanov and Margolina, 1996).

In this study, the Black Sea chlorophyll-*a* concentration data collected during the NATO SfP-971818 Project (in-situ data) are analyzed using the OSD method. The main purpose is to identify the basin-scale seasonal variability (one or two blooms?). The

rest of the paper is outlined as follows. Sections 2 and 3 describe the Black Sea oceanography and features of the in-situ chlorophyll-*a* observations. Section 4 depicts the framework of the OSD method and discusses its merits and limitations. Section 5 discusses the reconstructed chlorophyll-*a* field.

In Section 6, reliability of the reconstruction results is analyzed. The main conclusions are presented in
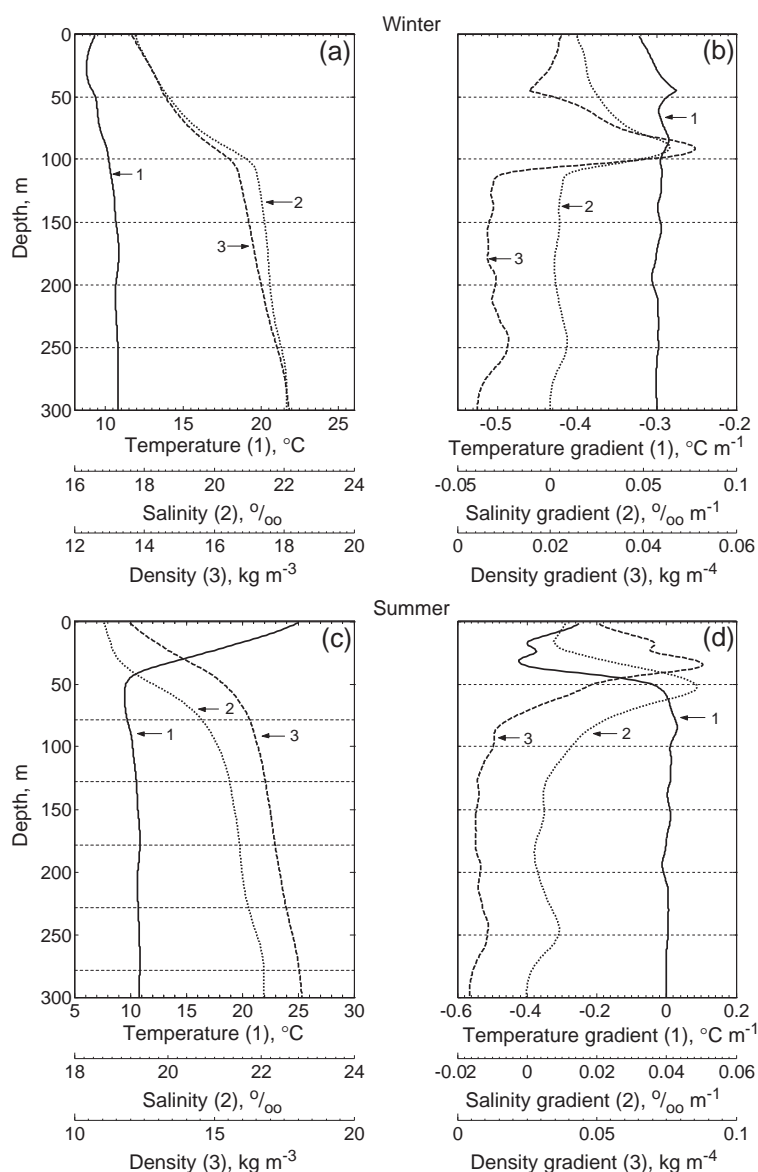

Fig. 2. The Black Sea temperature, salinity, and potential density profiles and their vertical gradients: (a) winter profiles, (b) winter vertical gradients, (c) summer profiles, and (d) summer vertical gradients.

Section 7. Appendix A provides discussion on the capability of the OSD to fill considerable spatial gaps in observation coverage.

2. Black Sea oceanography

The Black Sea is the largest inland basin in the middle latitudes with coastal and deep parts profoundly dissimilar to each other (Fig. 1). The deep basin with a relatively flat bottom (depth between 2000 and 2300 m) occupies more than 60% of the total area. The wide northwestern continental shelf with depth about 50 m takes most of the remaining area. Thus, interactions between coastal and deep ecosystems are inherent for the Black Sea. The basin-scale circulation appears as a cyclonic large-scale flow, the Rim Current. This jet-current is associated with two principal cyclonic gyres situated in the western and eastern parts of the basin, and anti-cyclonic eddies dominating the coastal zone (Fig. 1).

Hydrological balance of the Black Sea determines its hydrochemical structure. The Black Sea has a two-layer hydrographic structure. Cold and fresh surface layer water, which is controlled mainly by the riverine input, overlies warm and salt deep water, which is under the influence of inflowing salty Mediterranean water through the Bosphorus Strait. Thus, the density of subsurface water is determined mainly by the salinity. The halocline and pycnocline coincide at a depth between 100 (near the centers of the main cyclonic gyres) and 200 m (around the coastal margins).

Typical temperature and salinity profiles (Blatov et al., 1984) are shown in Fig. 2. The depth of the pycnocline overlaps with the lower boundary of the Cold Intermediate Layer extending over the entire deep-water area of the Black Sea. This layer has a temperature minimum (6.5–7.5 °C) between 25 and 150 m and considerably affects the hydrological, hydrochemical, and biological processes. The salinity stratification substantially governs the vertical exchange and as a result, causes the coincidence of the oxycline and chemocline at a depth between 100 and 200 m. The permanent presence of intense density stratification facilitates the formation of anoxic water masses below σ_θ=16.1–16.2 kg m^{-3}. On the other hand, the upper mixed layer of low salinity responds

strongly to seasonal heating and cooling and, as a result, the temperature predominantly determines the density in the summer season (Fig. 2b). From spring to fall, a shallow thermocline forms at a depth of about 30 m that is the upper boundary of the Cold Intermediate Layer. Obviously, the above description of the Black Sea is far from comprehensive. For more detailed information, the interested readers are referred to a more complete synthesis of the Black Sea oceanography (Murray, 1991; Ozsoy and Unluata, 1997).

Table 1
Sources of the utilized chlorophyll-*a* measurements

Month	Year	RV, cruise	Overall sampling size	Method
January	1986	PV, 20	18	Fl
	1988	PV, 25	46	Fl
	1992	PV, 36	5	Fl
February	1992	PV, 36	3	Fl
March	1986	PV, 20b	45	Fl
	1988	ML, 49	80	Fl
	1995	PK, 33	13	Fl
April	1988	PK, 18	33	Fl
	1989	PV, 28	4	Fl
	1993	PK, 30	10	Fl
	1993	PV, 41	37	Fl
	1995	PK, 33	13	Fl
May	1982	PV, 12	15	Sp
	1988	PK, 18	1	Fl
June	1989	PV, 28	36	Fl
	1991	PV, 33	44	Fl
July	1982	AT, 03/1	66	Fl
	1985	PV, 19	9	Fl
	1992	PV, 37	23	Fl
August	1980	PV, 9	21	Sp
	1982	AT, 03/1	14	Fl
	1990	PV, 32	9	Fl
	1992	PV, 38	7	Fl
September	1980	PV, 9	59	Sp
	1983	PK, 7	24	Fl
	1984	ML, 43-1	32	Fl
	1985	PK, 12-2	81	Sp
	1990	ML, 53a	16	Fl
	1991	PK, 28	36	Fl
October	1990	ML, 53a	65	Fl
	1991	PK, 28	10	Fl
November	1983	PK, 7	43	Fl
	1989	ML, 51	21	Fl
	1991	PV, 35	25	Fl
December	1987	PV, 25	16	Fl
	1989	ML, 51	14	Fl
	1994	PK, 32	71	Fl

3. Chlorophyll-*a* concentration data

Table 1 lists the in-situ chlorophyll-*a* measurements (1980–1995) from the NATO SfP-971818 ODBMS Black Sea Project. The data were collected during 26 expeditions of research vessels "Mikhail Lomonosov" (ML), "Ay-Todor" (AT), "Professor Kolesnikov" (PK) and "Professor Vodyanitsky" (PV) of the Ukrainian National Academy of Sciences (Marine Hydrophysical Institute and Institute of Biology of the Southern Seas, Sevastopol, Ukraine). The chlorophyll-*a* concentration was measured using fluorometric (Fl) and spectrophotometric (Sp) techniques. The accuracy of these measurements will be discussed in the next section.

The data set contains about 1100 chlorophyll-*a* concentration profiles from the surface to 100 m depth. They are sparse and irregular in time and space (Figs. 3
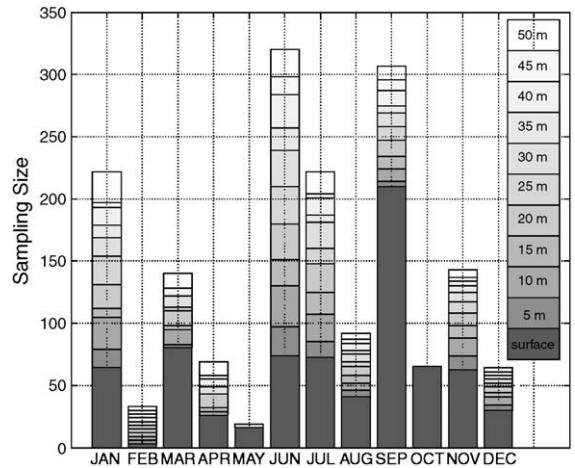

Fig. 4. Time (by month) and depth distribution of the observed chlorophyll-*a* observations.
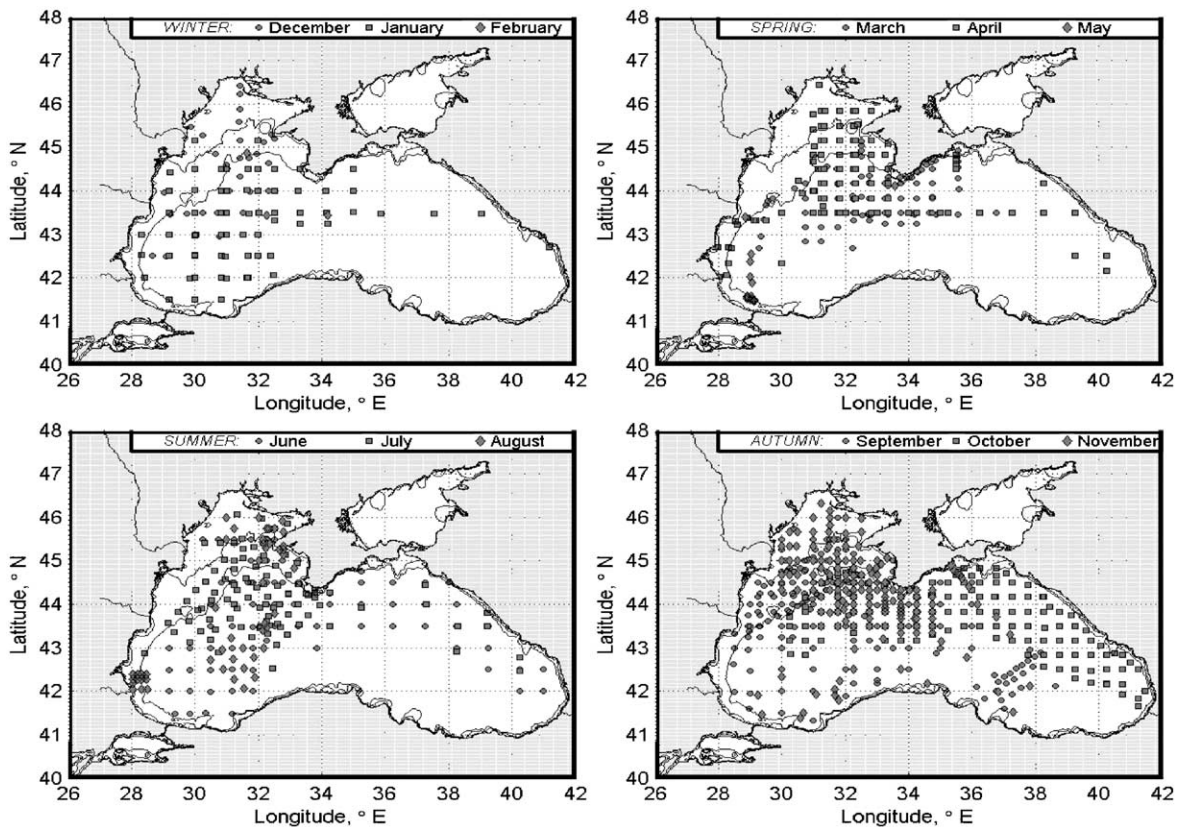

Fig. 3. Distribution of chlorophyll-*a* observational stations: (a) winter, (b) spring, (c) summer, and (d) fall.

and 4). Certain periods and areas are well sampled while others lack enough observations to gain any statistically meaningful estimates. For example, October and December have much fewer data points than the other months (Fig. 4). Even the months with a relatively large number of data have rather irregular sampling distribution in the horizontal and vertical.

4. Methodology

4.1. Removal of inter-annual trend

Since the main goal here is to estimate the seasonal variability of chlorophyll-a concentration, the interannual trend $c_{trend}(t)$ should be removed prior to the reconstruction,

$$c(\mathbf{x}, z, t) = c_{obs}(\mathbf{x}, z, t) - c_{trend}(t), \tag{1}$$

where $c_{obs}(\mathbf{x}, z, t)$ is the measured chlorophyll-a concentration at location $(\mathbf{x}, z)$ and time t. The Black Sea chlorophyll-a concentration does not have any evident interannual trend before 1988, and has distinct interannual trends between 1988–1992 and 1992–1995 (Yunev et al., 2002). The traditional approach (Saltzman, 1983) is used to estimate the interannual trends for the two periods 1988–1992 and 1992–1995,

$$c_{trend} = \begin{cases} a_0 + a_1 t, & t \in [1988, 1992] \\ b_0 + b_1 t, & t \in [1992, 1995] \end{cases}, \tag{2}$$

where $a_0 = -28.493$ mg m^{-3}, $a_1 = 0.014$ mg m^{-3} year^{-1}, $b_0 = 55.051$ mg m^{-3}, $b_1 = -0.0275$ mg m^{-3} year^{-1}.

4.2. Optimal spectral decomposition method

The OSD method was described in detail for closed (Eremeev et al., 1994, 1995; Ivanov and Margolina, 1996; Danilov et al., 1996; Chu, 1999; Ivanov et al., 2001, 2004; Chu et al., 2003a,b) and semi-closed basins (Chu et al., 2003a,b; Ivanov et al., 2004). Here, a brief description is given to illustrate the special features of the OSD method for analyzing the chlorophyll-a in-situ measurements in the Black Sea.

4.2.1. Spectral decomposition

The de-trended Black Sea chlorophyll-a concentration $c(\mathbf{x}, z, t)$ at depth z_k is decomposed using the generalized Fourier series (Ivanov et al., 2001)

$$c(\mathbf{x}, z_k, t) = A_0(z_k, t) + \sum_{m=1}^{M} A_m(z_k, t) \Psi_m(\mathbf{x}, z_k),$$
$$\mathbf{x} \in R(z_k) \tag{3}$$

where M is the truncated mode number, $\Psi_m(\mathbf{x}, z_k)$ and $A_m(z_k, t)$ are the orthogonal basis functions (or called modes) and the spectral coefficients, respectively; $R(z_k)$ is the area bounded by the Black Sea lateral boundary $\Gamma(z_k)$ at depth z_k.

The eigenfunctions $\{\Psi_m(\mathbf{x}, z_k)\}$ of the horizontal Laplace operator with the basin geometry and homogeneous Neumann boundary condition at $\Gamma(z)$ are taken as the basis functions,

$$\nabla_h^2 \Psi_m = -\lambda_m \Psi_m, \quad \mathbf{n} \cdot \nabla_h \Psi_m|_\Gamma = 0,$$
$$m = 1, 2, \ldots, M, \tag{4}$$

where $\nabla_h^2 \equiv \partial^2/\partial x^2 + \partial^2/\partial y^2$, and $\mathbf{n}$ is the unit vector normal to $\Gamma(z)$. The basis functions $\{\Psi_m\}$ are independent of the data and therefore available prior to the data analysis.

The OSD method has two important procedures: optimal mode truncation and determination of spectral coefficients $\{A_m\}$. After the two procedures, the generalized Fourier spectrum (3) is used to provide data at regular grids in space and time.

4.2.2. Optimal mode truncation

The optimal mode truncation number (M_{opt}) is defined as the critical mode number with the set of spectral coefficients $\{A_m\}$ least sensitive to observational data sampling and noise. For sample size of P and mode truncation of M, the spectral coefficients $\{A_m\}$ are estimated by the least square difference between observed and calculated values (Menke, 1984),

$$J_{emp} = J(\tilde{A}_1, \ldots, \tilde{A}_M, P, M)$$
$$= \frac{1}{P} \sum_{j=1}^{P} \left(c^{(j)} - \sum_{m=1}^{M} \tilde{A}_m(z, t) \Psi_m^{(j)}(\mathbf{x}, z) \right)^2 \rightarrow \min, \tag{5}$$

where the symbol "~" denotes the estimated values at location $(\mathbf{x}, z)$. For homogeneously sampled data with low noise and without systematic error, the empirical cost function J_{emp} should tend to 0 monotonically as M

increases to infinity. The set of the spectral coefficients $\{A_m\}$ depends on the mode truncation M. Optimal estimation of $\{A_m\}$ is equivalent to the determination of M_{opt} (Ivanov et al., 2001, 2004; Chu et al., 2003a,b).

A modified cost function (Vapnik and Chervonenkis, 1974a,b),

$$J \leq \frac{J_{emp}}{1 - \sqrt{\dfrac{M\left(\ln\dfrac{P}{M} + 1\right) - \ln(1 - \tau)}{P}}}. \tag{6}$$

is used to determine the optimal mode truncation M_{opt}. Here, τ is the probability of $|J - J_{emp}| \to 0$ as M increases. It is reasonable to take $\tau = 0.95$ (Mikhal'sky, 1987). Previous studies on the Black Sea chlorophyll-a and radionuclides Cs-137, Cs-134 and Sr-90 (Eremeev et al., 1994, 1995; Ivanov et al., 2001) show that M_{opt} is 30–50 for the basin-scale (~300 km) variability and 150 for the mesoscale (~20 km) variability. For sparse and noisy data, it is difficult to get reliable and stable estimates of all the necessary spectral coefficients, but the first six spectral coefficients $\tilde{A}_0(z_k,t)$, $\tilde{A}_1(z_k,t)$,..., $\tilde{A}_5(z_k,t)$ are reliable and stable. This is consistent with an earlier study (Ivanov et al., 2001). Since the first six modes represent neither basin-scale variability (30–50 modes required) nor mesoscale variability (150 modes required), the only physically realistic estimation is the horizontally averaged concentration $\bar{c}(z,t)$, which is $\tilde{A}_0(z_k,t)$.

4.2.3. Regularization procedure

Determination of the spectral coefficients is achieved by solving a set of linear algebraic equations of $\{\tilde{A}_m(z,t)\}$ that are obtained from the optimization procedures (3) and (6). Due to the high level of noise contained in the observations, the set of algebraic equations is ill-posed and needs to be solved by a regularization method that requires: (a) stability (robustness) even for data with high noise, and (b) the ability to filter out errors with a-priori unknown statistics. Numerical tests (Ivanov et al., 2001) on the reconstruction of the Black Sea June climatological chlorophyll-a concentration demonstrate the powerfulness of the technique on the basis of Eq. (6) in conjunction with Tikhonov's-like regularization procedures (Tikhonov et al., 1990) and the rotation matrix method (Chu et al., 2004).

4.3. Filling of temporal gaps

Because of the data sparseness and irregularity (Fig. 4), the horizontally averaged concentration $\bar{c}(z_k,t_i)$ [i.e., $\tilde{A}_0(z_k,t)$] is directly calculated only for the following nine months: January, March, April, June, July, August, September, October (only for the sea surface) and November. The Fourier series expansion is used to find the values for other months,

$$\bar{c}(z_k, t_i) = a_0(z_k) + \sum_{l=1}^{L} [a_l(z_k)\cos(l\omega t_i) + b_l(z_k)\sin(l\omega t_i)], \tag{7}$$

with $L=3$, $\omega = 2\pi/T$, and $T=12$ months. The seven spectral coefficients a_0, a_l and b_l ($l=1, 2, 3$) are calculated from the data $[\tilde{A}_0(z_k,t)]$ using the least square principle with a natural a-priori constraint,

$$\bar{c}(z_k, t_i) > 0.$$

4.4. Reconstruction skill

Clearly, reconstruction of the Black Sea chlorophyll-a concentration from noisy and sparse in-situ data is an ill-posed problem. The OSD method has the following merits.

(i) *Robustness*. The reconstructed monthly mean Black Sea chlorophyll-a concentration is robust to variation of the observational sampling and small perturbations of the measurements (property of any regularized estimates (Tikhonov et al., 1990). In many cases, the regularized estimations are insensitive to large observation errors (Chu et al., 2004). For observations with white Gaussian noise, the vertical structure of the monthly mean Black Sea chlorophyll-a concentration can be reconstructed even with high noise-to-signal ratios such as 2–4.

(ii) *Positiveness*. The chlorophyll-a concentration must be positive. This is a very strong a-priori constraint to filter numerous unrealistic solutions.

(iii) *Statistical completeness*. The spectral coefficients $\tilde{A}_m(z,t)$ tend to the true values without

any discontinuity as the observations increase to infinity (Vapnik and Chervonenkis, 1974a,b). This property is automatically preserved using the cost function (6) if no systematic error exists in the observations.

4.5. Sources of reconstruction errors

Three sources of uncertainty exist in reconstructing the chlorophyll-*a* concentration: (a) measurement errors, (b) unresolved-scale errors caused by sparse and irregular sampling.

4.5.1. Measurement errors

In the in-situ chlorophyll-*a* concentration data, approximately 30% of the measurements use the standard SP method (Jeffrey and Humphrey, 1975), and about 70% of the measurements use the FL method (Lofrus and Carpenter, 1971). After comparing the accuracy of the two methods from R/V "Professor Vodyanitsky" during March–April 1999, Yunev et al. (2002) found that the maximum relative difference of the chlorophyll-*a* concentrations measured by the two methods is less than 19%. This allows us to collect all the measurements in a single data set without any preliminary correction.

Individual chlorophyll-*a* concentration measurement error varies in space (from station to station) and time. The chlorophyll-*a* signals are mixed with the accessory pigments (chlorophyll-*b* and chlorophyll-*c*) and the degradation products (pheophytin-*a*, pheophytin-*b* and pheophytin-*c*) (Hallegraeff and Jeffrey, 1985; Moberg et al., 2001). These pigments and pheopigments are interfering compounds in the SP and FL methods because they absorb and fluoresce at the same wavelengths as the chlorophyll-*a* (Lorenzen and Jeffrey, 1980). However, the error estimation for this case is poorly documented.

Measurements in the Black Sea (Vedernikov and Demidov, 1997) and the Indian, Pacific and Atlantic Oceans (Trees et al., 1985) show that the SP method overestimates the chlorophyll-*a* concentration by about 60%; and the FL method underestimates the chlorophyll-*a* concentration by about 30%. The mean measurement error ranges between about 40% and 50% from station to station. As a working hypothesis, the measurement error is assumed to be Gaussian white noise $(0, \sigma)$ in space and time. The noise spectrum associated with the measurement error is represented by (Sabel'feld, 1991)

$$\langle B_m^2 \rangle = \frac{\sigma^2}{M_0}, \tag{8}$$

where M_0 (~300) is the spectral mode analogue to the Nyquist frequency of a regular discrete time series. For two-dimensional sampling, the wavelength $L_0 = M_0^{-1}L$ has the order of "twice the averaged station separation". Here, L is the integral horizontal scale of the Black Sea.

The variance of the reconstructed chlorophyll-*a* concentration field is represented by the Euclidean norm $||\delta A_m^2||_{m=1}^{M_{opt}}$. The variance of noise in the input signal is estimated by

$$\sigma_{error}^2 = \sigma^2 M_{opt}/M_0 \sim 1.2 \times 10^{-2}, \tag{9}$$

which shows that the optimal mode truncation M_{opt} reduces drastically the impact of measurement noise on the reconstruction accuracy.

4.5.2. Unresolved-scale errors

The second error source is unresolved synoptic and mesoscale motions. The Black Sea has strong mesoscale and synoptic variability, such as in the Rim current on the shelves (Ozsoy and Unluata, 1997; Oguz et al., 2002a), that greatly affects the spatial and temporal variability of chlorophyll-*a* concentration. Based on numerical simulation and analysis of the SeaWiFS images, Oguz and Salihoglu (2000) show that the mesoscale features can control patchiness and intensity of chlorophyll-*a* concentration ranging between 1 and 3 mg m^{-3} during the spring bloom. As the first guess, we may parameterize this variability as red noise with a correlation radius R_{cor} (Thiebaux and Pedder, 1987).

Twin experiments show weak sensitivity of the reconstruction skill of a scalar field in the Black Sea to the correlation radius of the unresolved-scale processes represented by the Gaussian red noise if $R_{cor} \leq 2L_0$ (Ivanov et al., 2001). The reconstruction error grows approximately linearly for large correlation scales. If the Rossby deformation radius R_d (around 35–40 km for the Black Sea) is used to represent the correlation radius ($R_{cor} \sim R_d$), then R_{cor} is much smaller than $2L_0$. Therefore, the variability with

such spatial scales should be effectively filtered by the regularization procedure.

It is more difficult to evaluate the impact of unresolved-scale errors on the reconstruction skill than of measurement errors. Usually, the unresolved-scale error variance is assumed to be 30–50 times the measurement error variance σ^2 (Thiebaux and Pedder, 1987), which leads to 40–60% error variance distorting the input signal.

The regularization guarantees an accuracy around 20–30% of the norm $||\delta A_m^2||_{m=1}^{M_{opt}}$ utilizing the observational data with 40–60% error variance (Ivanov et al., 2001; Chu et al., 2003a,b). Thus, 20–30% can be taken as the low accuracy limit in estimating $\tilde{A}(z_k,t)$ [i.e., $\bar{c}(z_k,t_i)$].

4.5.3. Irregular sampling errors

Irregular sampling is also a major source of uncertainty. The OSD method is sufficient to filter out errors if the characteristic spatial scale of the reconstructing field L_0 is twice the characteristic scale of the observational gaps L_{gap}. In estimating $\tilde{A}(z_k,t)$, the reconstruction procedure was proved efficient (Ivanov et al., 2001) through reconstructing horizontal mean Black Sea scalar fields with various sampling strategies.

5. Seasonal variability

Horizontally averaged chlorophyll-*a* concentrations in the Black Sea, $\bar{c}(z_k,t_i)$, are calculated using the OSD method [i.e., $\tilde{A}(z_k,t)$, Fig. 5a] and the simple arithmetic mean (in the horizontal and month) of the in-situ chlorophyll-*a* concentration data (Vedernikov and Demidov, 1997, hereafter called the VD97 profiles, Fig. 5b) at 11 depths z_k [$k=1$, K, $K\equiv11$] between the sea surface and 50 m depth with 5-m interval. There are 11 VD97 profiles for all months except December. The distinction between the two is
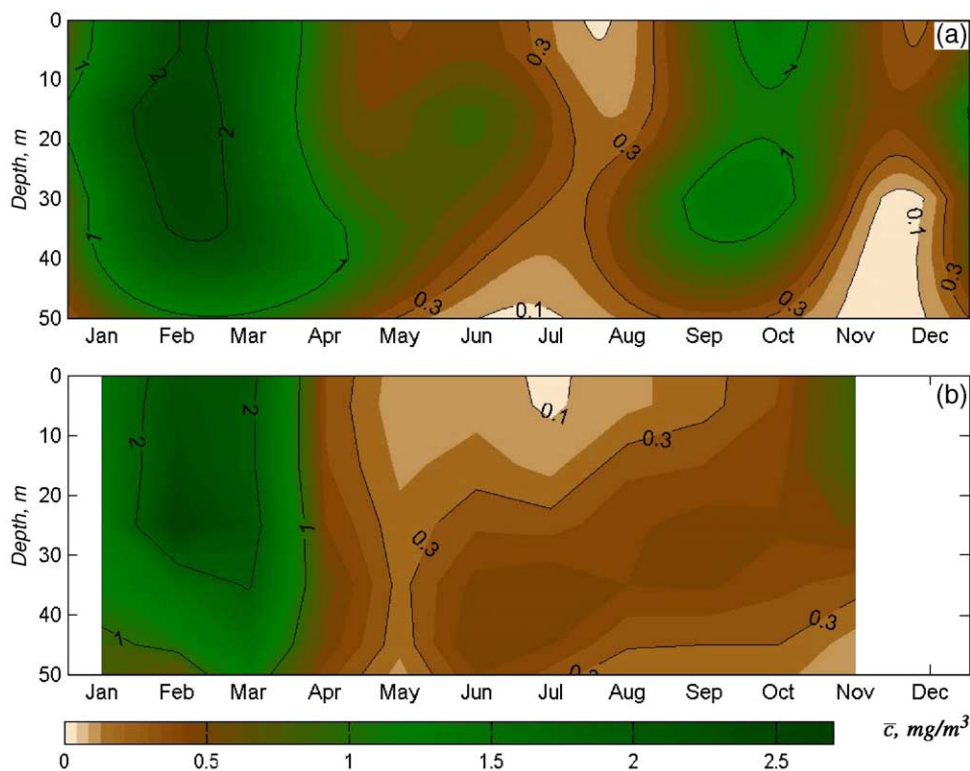

Fig. 5. Time-depth cross-sections of $\bar{c}(z,t)$ from (a) the OSD reconstructed field with two blooms in February/March (winter/spring bloom) and September/October (fall bloom), (b) the VD97 profiles with only one bloom in February/March (winter/spring bloom).

the two-bloom structure (winter/spring and fall) in the reconstructed field (OSD method) versus one-bloom structure (winter/spring) in the VD97 profiles. The seasonal variability identified using the OSD method is described below.

Sufficient nutrient supply, light availability, and biological interaction might trigger a bloom. Sverdrup (1953) defined a critical depth above which the depth-integrated daily gross primary production equals phytoplankton loss through grazing and respiration. The critical depth is associated with the light availability and deepens in spring and summer.

During the winter season, intensive mixing provides the upper layer with nutrients but the phytoplankton production remains low because of light limitation. The winter/spring bloom occurs in February/March with a maximum value of 2.25 mg m^{-3}. This period is characterized by near uniform chlorophyll-*a* distribution within the mixed layer (30 m depth), which is shallower than the critical layer depth. Phytoplankton transport to below the critical depth is prevented and the majority of the phytoplankton remains within the euphotic zone. This mechanism in combination with the nutrient abundance triggers the winter/spring bloom which continues until nutrient depletion occurs in the upper layer.

At the end of April, spring bloom terminates as a result of depletion of the nitrate stock and/or increasing role of the grazing pressure imposed by the growing zooplankton community. The near surface chlorophyll-*a* concentration decreases, but the subsurface chlorophyll-*a* maximum exists almost all the time, except in November, with varying depth and intensity. Depth of the chlorophyll-*a* maximum (exceeding 0.6 mg m^{-3}) is localized between 15 and 20 m in late spring/early summer. In early fall, it dips to 25–35 m depth and intensifies by nearly a factor of two. During all of the warm period from May till September, the phytoplankton production in the surface layer remains low because of nutrient limitation even though the light conditions are favorable for photosynthesis.

Towards the end of September, the surface chlorophyll concentration begins to increase again and reaches its second maximum in October. The fall bloom has half the intensity of the winter/spring bloom and is restricted within the upper 10 m only. The surface (above 10 m) and subsurface (below 20 m) chlorophyll-*a* concentration maxima (>1.0 mg m^{-3}) are

isolated by relatively low concentrations ranging between 0.5 and 1 mg m^{-3}.

Like the winter/spring bloom, the fall bloom is mainly driven by the mixing processes in the Black Sea. As vertical mixing intensifies in the early fall, the seasonal thermocline starts to erode and favors the vertical transport of nutrients from deep to surface waters and of phytoplankton to depth with favorable insolation conditions. Oguz et al, (2000, 2003) pointed out that the fall bloom is governed not only by physical processes but also by biological interactions within the Black Sea environment, such as fall rebounds in gelatinous carnivore populations and subsequent decreases in herbivorous mesozooplankton stocks.

The two maxima (winter/spring and fall) and one minimum in the summer are generally recognized as a natural pattern of the phytoplankton annual cycle in middle latitudes (Longhurst, 1995; Sathyendranath et al., 1995). Physically driven (wind-induced, fronts, upwelling) water mixing drives seasonal nutrient supply to the euphotic zone, and in turn causes the primary production (Longhurst, 1995). In addition to this "bottom-up" forcing, "top-down" control by the gelatinous predators plays a remarkable role in the Black Sea phytoplankton distribution and evolution on the basin scale. This was confirmed in numerical simulations using a one-dimensional, vertically resolved, coupled physical biochemical model (Oguz et al., 2000).

6. Subsurface chlorophyll-*a* maximum

The reconstructed data (OSD method) show that the subsurface chlorophyll-*a* maximum is located at 40 m depth in April and 35 m depth in August (Fig. 6a), occurring just after the winter/spring bloom and shortly before the fall bloom. The shoaling of the chlorophyll-*a* maximum occurs in June (15 m) and in December–February (15 m) between the two deepening events (in April and August) and is accompanied by a continuous reduction of subsurface maximum chlorophyll-*a* concentration (Fig. 6b). The subsurface maximum peaks at 2.25 mg m^{-3} in February and peaks again at 1.16 mg m^{-3} in September–October. Two minima occur 0.40 mg m^{-3} in July and 0.58 mg m^{-3} in December.

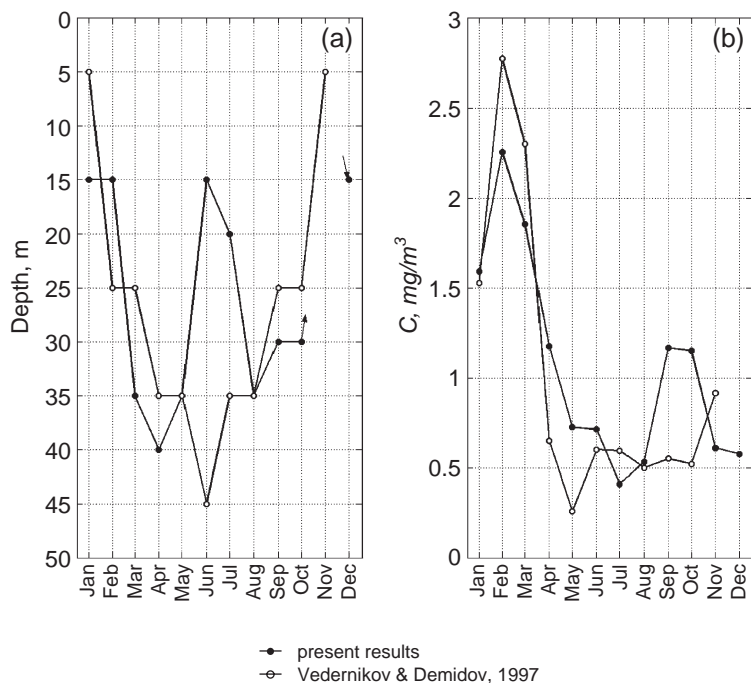The VD97 profiles show that the subsurface chlorophyll-*a* maximum is located at 5 m depth in

Fig. 6. Monthly mean (a) subsurface chlorophyll-*a* maximum depth, and (b) subsurface chlorophyll-*a* maximum concentration, estimated using OSD (dotted) and simple arithmetic mean (Vedernikov and Demidov, 1997) (circle).

the winter (November–January) and 45 m in June (Fig. 6a). The subsurface chlorophyll-*a* concentration in this data set has one maximum of 2.75 mg m^{-3} in February and one minimum of 0.25 mg m^{-3} in May (Fig. 6b).

Two major discrepancies are found between the reconstructed and VD97 profiles: (a) the subsurface chlorophyll-*a* concentration in September–October is 1.16 mg m^{-3} in the reconstructed profiles and 0.50–0.55 mg m^{-3} in the VD97 profiles, and (b) the depth of the subsurface chlorophyll-*a* maximum in June is 15 m in the reconstructed profiles and 45 m in the VD97 profiles.

In the fall (September–October), the depth of the subsurface chlorophyll-*a* maximum is 25 m in the reconstructed profiles and 30 m in the VD97 profiles, both occur in the upper mixed layer with favorable photic conditions. These conditions may favor the existence of the second maximum in the subsurface chlorophyll-*a* concentration.

In June, whether the true depth of the subsurface chlorophyll-*a* maximum is shallow (15 m) or deep (45 m) can be evaluated using the existing analysis and data. Based on the data collected during the last 20

years, Yunev et al. (1999) show the existence of four major types of chlorophyll-*a* concentration profiles. According to their classification, one well advanced and symmetric maximum or two and more maxima, which are comparable or differing in magnitude, are characteristic features of the vertical distribution of chlorophyll-*a* during summer and autumn when the temperature stratification is a barrier to penetration of additional nutrients from the bottom layers into surface layer. For example, two in-situ measured chlorophyll-*a* concentration profiles (Fig. 7) clearly indicate the existence of a chlorophyll-*a* maximum at nearly 20 m depth (Oguz et al., 1999).

The location and intensity of the subsurface chlorophyll-*a* maximum in the Black Sea are governed by nutrient availability in the euphotic zone (Yunev et al., 1999). The winter/spring high primary production causes subsequent depletion of the nutrients in the surface layer, but not in the thermocline. This increases the chlorophyll-*a* concentration in the algal cells and population of phytoplankton in the thermocline, and establishes the subsurface chlorophyll-*a* maximum in the stratified
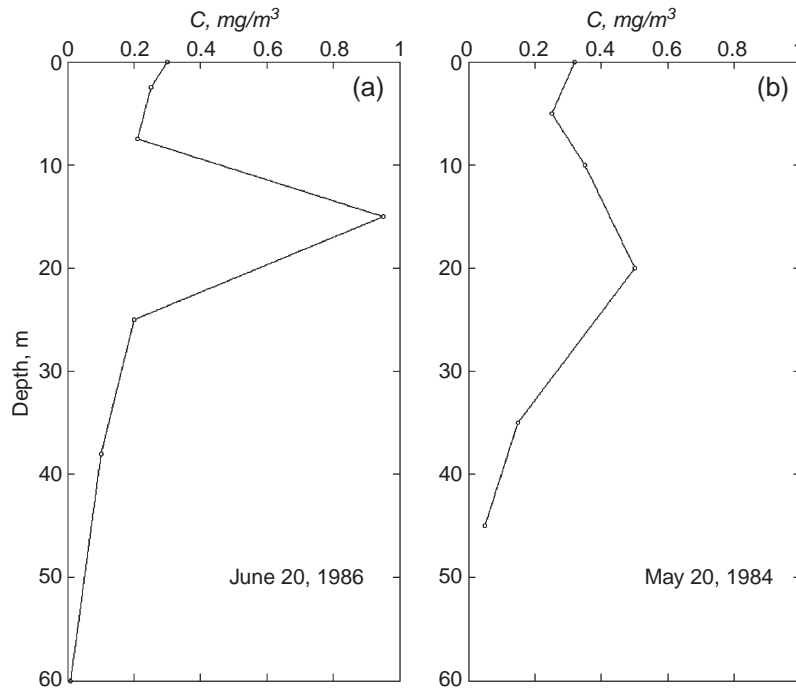
Fig. 7. Two observed summer vertical profiles of chlorophyll-*a* in the Black Sea: (a) June 20, 1986, and (b) May 20, 1984.

ocean (Kirk, 1983). Thus, the subsurface chlorophyll-*a* maximum should be located just below the seasonal thermocline. On the other hand, the layer of the chlorophyll-*a* abundance is restricted by the upper boundary of the permanent pycnocline. In June, the upper boundary of seasonal thermocline (permanent pycnocline) is 10 m (49–52 m) for the central western (Fig. 8a) and eastern (Fig. 8b) cyclonic gyres. The estimated depth of the subsurface chlorophyll-*a* maximum in June in the reconstructed profiles (15 m) is more realistic than in the VD97 profiles (45 m).

7. Total chlorophyll-*a* amount

Vertical integration of $\tilde{A}(z_k,t)$ (i.e., estimation of the horizontally averaged chlorophyll-*a* concentration) from the sea surface to 50 m depth, $Q_{50}(t_i)$ is taken as the monthly mean total chlorophyll-*a* amount with the annual mean

$$\langle Q_{50} \rangle = \frac{1}{T} \int_0^T Q_{50}(t) \mathrm{d}t \approx 0.40 \ \text{g Chl m}^{-2}, \qquad (11)$$

and variance

$$\langle \delta Q_{50}^2 \rangle = \frac{1}{T} \int_0^T (Q_{50} - \langle Q_{50} \rangle)^2 \mathrm{d}t \approx 0.07 \ (\text{g Chl})^2 \ \text{m}^{-4}.$$

$$(12)$$

The total chlorophyll-*a* amount $Q_{50}(t_i)$ from the reconstructed data (Fig. 9) has two maxima occurring in February [1.00 g (Chl) m^{-2}] and September/October [0.48 g (Chl) m^{-2}] and two minima occurring in July–August and November–December [0.1 g (Chl) m^{-2}]. The variability indices (i.e., ratio of maximum to minimum) are 9.9 and 4.9 for the two cycles, respectively. The monthly mean phosphate and depth of the photosynthetic layer are also plotted in Fig. 9 to help understand the phytoplankton dynamics using the abiotic factors.

The phosphate concentration has a maximum [0.77 μmol (P) l^{-1}] in February. The available nutrients have been transported to the upper layer in the winter due to the intensive mixing processes. With the shoaling of the permanent pycnocline to about 30
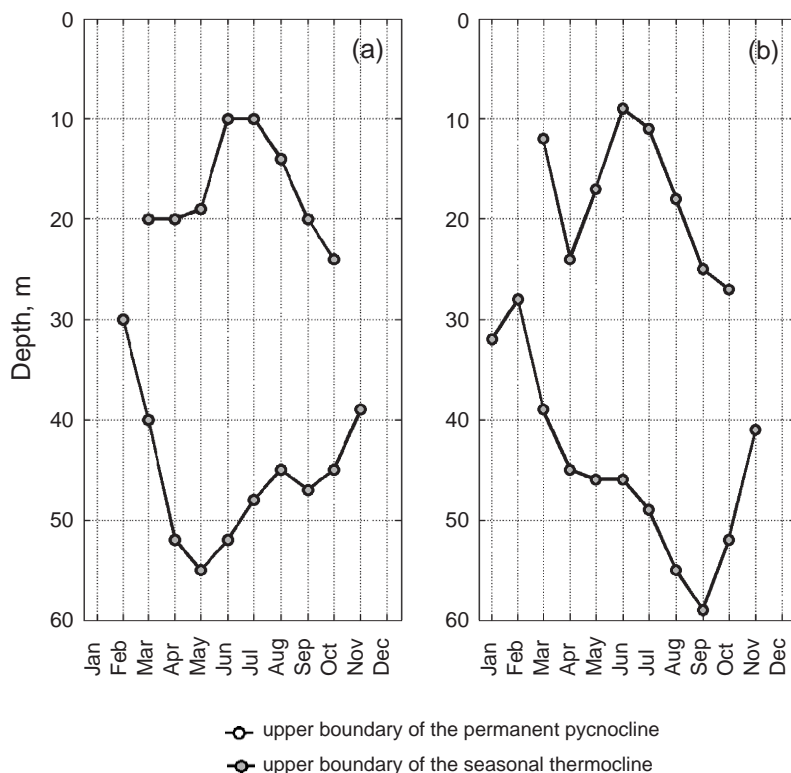
Fig. 8. Upper boundaries of the permanent pycnocline and seasonal thermocline in the (a) western and (b) eastern cyclonic gyres.

m, the phytoplankton remain in the euphotic zone with the shallowest depth of 30 m. This causes the major bloom in February.

After the winter/spring bloom, the upper layer total chlorophyll-*a* amount reduces rapidly to 0.27 g (Chl) m^{-2} in May because of nutrient limitation despite a
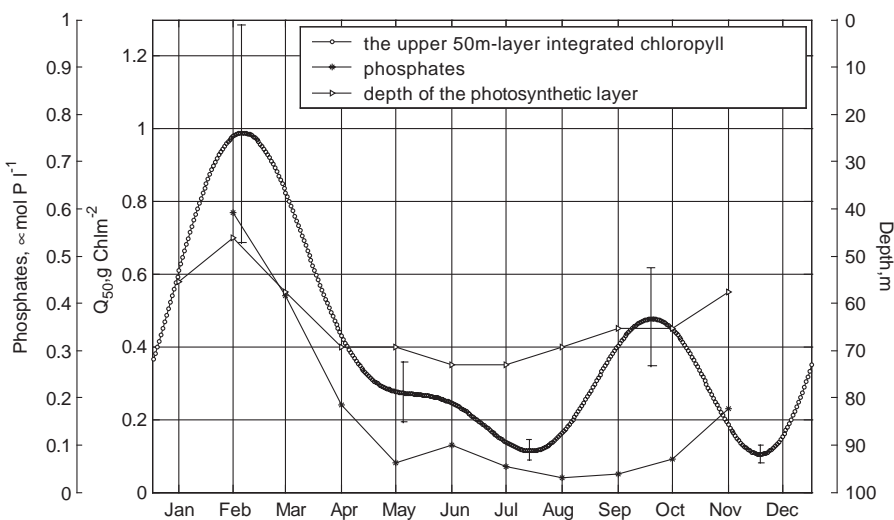

Fig. 9. OSD reconstructed monthly mean Q_{50} with error bars.

favorable combination of increased daily insolation and onset of thermal stratification. From May to June (early summer), the rate of this reduction slows down possibly due to the intensification of the subsurface chlorophyll-*a* maximum, which was discussed in the previous section.

In July/August, the upper layer total chlorophyll-*a* amount $Q_{50}(t_i)$ starts to increase and reaches its second maximum value [0.48 g (Chl) m^{-2}] by October, associated with the fall bloom. The strength of the fall bloom is nearly half that of the winter/spring bloom. During that period, the seasonal thermocline starts to erode because of the strong surface atmospheric forcing, which is followed by the nutrient upwelling and phytoplankton rising to depths of favorable insolation conditions.

8. Significance of the fall bloom

The Black Sea has poor data coverage of the chlorophyll-*a* concentration in February and October, except at the surface (Table 1 and Fig. 4). But the reconstructed chlorophyll-*a* field shows the blooms during these months. The poor data average may raise

reasonable doubts about the reliability of the reconstructed field. To show the effectiveness and stability of this temporal interpolation scheme, the seven spectral coefficients $\{\tilde{a}_0, \tilde{a}_l, \tilde{b}_l | l=1,2,3\}$ in Eq. (7) are calculated in the upper 5-m layer, $\tilde{A}_0(z \geq -5 \text{ m}, t_i)$, from (a) all the available data, and from excluding the data measured in (b) April, and (c) August with the constraint, $\bar{c}(z_k, t_i) \geq 0$ (Fig. 10).

The two blooms (winter/spring and fall) exist in all three reconstructed sets and little difference is found among them. The difference is very small comparing (a) and (b), and is less than 12% for the winter/spring bloom and less than 30% for the fall bloom between using (a) and (c). The ratio of the first-to-second maximum chlorophyll-*a* concentration is 1.8, 2.2 and 2.3 for the three data sets. The stability of the reconstructed chlorophyll-*a* seasonal variability shows the power of the Fourier series expansion to effectively obtain the seasonal variability (two blooms) using temporally interrupted data. Although it has been identified using the SeaWiFS chlorophyll data (Oguz et al., 2002a,b), the fall bloom (September–October) in the Black Sea is first detected in this study using the in-situ measurements with insufficient sampling in this season.
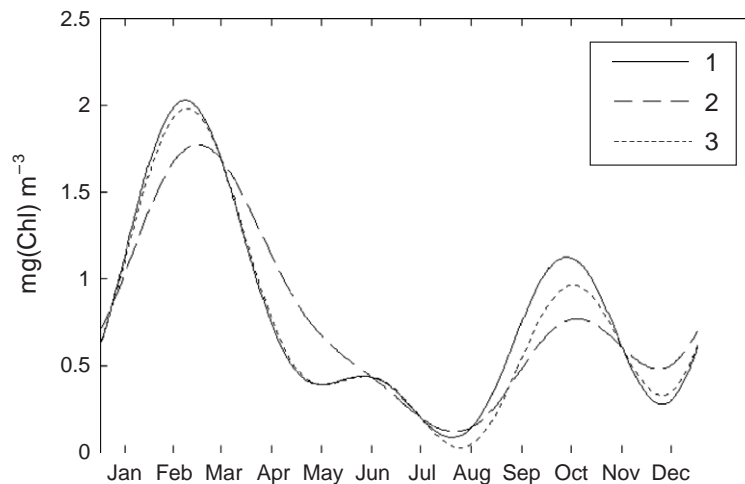

Fig. 10. Sensitivity of OSD reconstruction of the upper layer (within 5 m depth) chlorophyll-*a* concentration to temporal interruption using all available data (solid curve), data excluding April (dashed curve), and data excluding August (dotted curve).

9. Sensitivity to sampling size

The data for VD97 profiles were collected at 16 expeditions from 1978 to 1992. The data for Yunev et al.'s (2002) estimation contain about 1000 observations in the deep region of the Black Sea in 1964, 1973, 1978, and from 1980 to 1996. The data for this study contain about 1100 stations from 26 cruises in 1980–1995 (around 70% of all the existing chlorophyll-*a* concentration data) and coincide partially with the two earlier studies.

Since not all the Black Sea chlorophyll-*a* observational data are available for this study (as well as for others), sensitivity of the reconstruction to the sampling size of our data set was investigated. The results show that a reduction of 10–15% in sampling size affects the estimation of the monthly mean chlorophyll-*a* concentration slightly. However, the sampling size cannot be reduced any more than 10–15%, since further reduction will impair the filtering capabilities.

10. Effect of shelf data

Vedernikov and Demidov (1997) and Yunev et al. (2002) utilized the in-situ data for the deep basin of the Black Sea only (with water depth larger than 200 m). In the present study, we use the in-situ data on the northwestern shelf of the Black Sea along with the deep-basin data. Since the purpose of this research is to estimate the seasonal variability of horizontal mean chlorophyll-*a* concentration, it is necessary to assess the effect of the shelf data.

The effect of the shelf data on the seasonal variability of the horizontal mean chlorophyll-*a* concentration is significant using the simple arithmetic mean (the VD97 approach), and insignificant using the OSD method. This is because the truncated expansion (Eq. (3)) contains various horizontal scales of the chlorophyll-*a* field with the mode-0 representing the horizontal mean field. The first 30–50 modes represent the basin-scale (300 km) variability, and the first 150 modes represent the mesoscale (20 km) variability including the variability on the northwestern Black Sea shelf. Low-order truncation (at mode-5 in this study) automatically removes the effects of smaller scale (smaller than the basin-scale) processes including the mesoscale processes on the northwestern Black Sea shelf.

Let Q_{d+s} and Q_d be the horizontally averaged vertical integrations (0–5 m depth) of the chlorophyll-*a* concentration over the whole domain and the deep-basin only. The ratio Q_d/Q_{d+5} represents the effect of the shelf data with little effect if $Q_d/Q_{d+5} \sim 1$, and huge effect if $Q_d/Q_{d+5} \sim 0$. The ratio for the September chlorophyll-*a* field is 0.89 using the OSD method and 0.30 using the simple arithmetic method. This shows the capability of the OSD method to filter processes with scales smaller than the basin-scale.

11. Conclusions

(1) Noisy, sparse, and irregularly distributed chlorophyll-*a* concentration data collected in the Black Sea (including shelf waters) between 1980 and 1995 are analyzed using the OSD method. The reconstruction results present the depth-resolved annual variations of the horizontally averaged chlorophyll-*a* concentration within the upper 50-m layer.

(2) The reconstructed chlorophyll-*a* concentration shows the existence of two blooms with a strong winter/spring bloom [up to 2.00 mg (Chl) m^{-3}] in February/March and a less strong fall bloom [around 1.00 mg (Chl) m^{-3}] in September/October. The subsurface chlorophyll-*a* concentration also has a bi-modal temporal structure: two maxima, with the first maximum of 2.25 mg m^{-3} in February and the second maximum of 1.16 mg m^{-3} in September–October, and two minima, with the first minimum of 0.40 mg m^{-3} in July and the second minimum of 0.58 mg m^{-3} in December.

(3) The depth of the subsurface chlorophyll-*a* maximum has two maxima and two minima. The first maximum depth is 40 m in April, occurring just after the winter/spring bloom, and the second maximum depth is 35 m in August, appearing shortly before the fall bloom. The minimum depth is 15 m, occurring in December–February and June. The noticeable rise of the chlorophyll-*a* enriched zone in June between the two deepening events (in April

and August) is accompanied by a near-continuous reduction of upper 50-m layer chlorophyll-*a* concentration.

(4) The winter/spring bloom is the most prominent signal in the in-situ measurements of chlorophyll-*a* concentration and was identified using a simple arithmetic averaging procedure. This bloom is caused by sufficient nutrients being transported to the upper layer during the winter due to intensive mixing processes and a mixed layer depth shallower than the critical depth during the winter/spring period due to a decrease of the mixed layer depth and an increase of the critical depth.

(5) The fall (September/October) bloom was detected from the SeaWiFS images and reproduced in coupled physical–biological models, but cannot be identified from the in-situ measurements using the simple arithmetic averaging procedure. This study using the OSD method is the first time to identify the fall bloom in the Black Sea from the in-situ data.

(6) The OSD method is a useful alternative for the popular optimal interpolation method in marine data analysis with unknown first guess field and autocorrelations and high noise-to-signal ratio.

(7) Mechanisms explaining the existence of two blooms and the characteristics of subsurface chlorophyll-*a* maximum in the Black Sea should be further investigated utilizing additional information on various abiotic factors that affect the phytoplankton dynamics.

Acknowledgments

Appendix A. Representation of basin-scale field using sub-area data

The spatial distribution of the chlorophyll-*a* observations is heterogeneous with much less coverage over the eastern than the western Black Sea (Fig. 3). Why does the reconstructed horizontally averaged chlorophyll-*a* field represent the whole Black Sea when the east Black Sea is poorly sampled?

The spectral coefficients $\{A_m\}$ in the Fourier series (3) can only be approximately estimated due to the existence of noise,

$$A_m = \bar{A}_m + \delta A_m,$$

where $\{\bar{A}_m\}$ are the "true" coefficients, and $\{\delta A_m\}$ are errors. The total error is computed by

$$Q = \sum_{m=1}^{\infty} (\delta A_m)^2,$$

which should not be greater than the tolerance δ^2,

$$Q \leq \delta^2.$$

If the basis functions $\{\Psi_m\}$ are the eigenfunctions of the Laplacian operator, the Fourier series (3) is uniformly convergent (Morse and Feshbach, 1953) and the following theorem exists.

Theorem. If the Fourier series (3) converges uniformly and

$$\delta^2 M(\delta) \to 0 \quad \text{as} \quad \delta \to 0$$

then for any spatial point $x,y \in S$,

$$\lim_{\delta \to 0} \left| c(x,y,z,t) - \sum_{m=0}^{M(\delta)} A_m(t) \Psi_m(x,y,z) \right| \to 0, \qquad (A1)$$

which shows that the truncated mode number $M(\delta)$ always exists and determination of $M(\delta)$ strongly depends on the observation error. For homogeneously convergent Fourier series, the spectral coefficients $\{A_m\}$ may also be determined from a sub-area,

$$\oint_{S_0} \left(c - \sum_{m=1}^{M} A_m \Psi_m \right)^2 \mathrm{d}s \to \min, \qquad S_0 \subset S, \qquad (A2)$$

where S is the total area and S_0 is an arbitrary area where the data are collected. This theorem was proved by Tikhonov et al. (1990) and is only valid if the basis functions $\{\Psi_m\}$ are the eigenfunctions of the Laplace operator. It may not be valid if the basis functions $\{\Psi_m\}$ are empirical orthogonal functions because

they are not homogeneously convergent. For accurate observations (without noise and systematic error), it is sufficient to use sub-area data to reconstruct a field for the entire region.

Two remarks should be noted before using this theory. First, observational data are noisy and usually obtained from non-uniform sampling. The spectral coefficients are approximately estimated and the reconstructed field may not be accurate. The farther the location from the observational sub-area, the larger is the reconstruction error (large or even negative values of concentration) may occur. Second, the spatial scale of the field L determines the number of modes $\tilde{M}$ required for mode truncation. Since $M(\delta)$ in Eq. (A1) depends functionally on δ, it is true that $\tilde{M} > M$ for high noise and/or non-uniform sampling. That is to say that the mode truncation may not be totally determined from observations. If the truncation is at the mode-M, the reconstructed field has noticeable distortion in sub-areas with no observation.

Ivanov et al. (2001) use Black Sea twin experiments to examine the effect of noise and sampling strategy on the reconstruction quality using four nondimensional ratios: (1) noise-to-signal ratio (η_1) computed for areas containing observations; (2) mode number-to-observational number ratio (η_2), (3) reconstruction error-to-signal ratio for areas containing observations (E_1), and (4) reconstruction error-to-signal ratio for areas containing no observations(E_2). Here, η_1 represents the noise, η_2 the sampling strategy, and (E_1, E_2) the reconstruction errors.

For a Black Sea basin-scale scalar field, 30–50 modes should be used. If the measurement errors are represented by Gaussian white noise with $\eta_1 \leq 1$, and $\eta_2 \leq 0.1$, the reconstruction errors are estimated as

$$E_1 < 0.05, \quad E_2 < 0.25.$$

For the same conditions, but assuming Gaussian red noise with the correlation radius equivalent to the Rossby radius of deformation (40 km), the reconstruction errors are estimated as

$$(E_1, \ E_2) \simeq 0.20 - 0.25.$$

These estimations show that the reconstructed horizontally averaged chlorophyll-a field can repre-

sent the whole Black Sea when the east Black Sea is poorly sampled.

References

Blatov, A.S., Bulgakov, N.P., Ivanov, V.A., Koserev, A.N., Tuzhilkin, V.S., 1984. Variability of hydrophysical fields in the Black sea. Hydrometeoizdat. Leningrad. 240 pp.

Chu, P.C., 1999. Fundamental circulation functions for the determination of open boundary conditions. Proceedings of the Third Conference of Coastal Oceanic and Atmospheric Prediction. American Meteorological Society, Boston, MA, pp. 389–394.

Chu, P.C., Ivanov, L.M., Korzhova, T.P., Margolina, T.M., Melnichenko, O.M., 2003a. Analysis of sparse and noisy ocean current data using flow decomposition: Part 1. Theory. Journal of Atmospheric and Oceanic Technology 20, 478–491.

Chu, P.C., Ivanov, L.M., Korzhova, T.P., Margolina, T.M., Melnichenko, O.M., 2003b. Analysis of sparse and noisy ocean current data using flow decomposition: Part 2. Application to Eulerian and Lagrangian data. Journal of Atmospheric and Oceanic Technology 20, 492–512.

Chu, P.C., Ivanov, L.M., Margolina, T.M., 2004. Rotation method for reconstructing process and field from imperfect data. International Journal of Bifurcation and Chaos 14 (8), 2991–2997.

Danilov, A.I., Ivanov, L.M., Kulakov, M.Yu, Margolina, T.M., Pavlov, V.K., 1996. Modern radioactive climate of the Kara Sea. Geophysical Report, Russian Academy of Sciences 346 (4), 545–548 (in Russian).

Eremeev, V.N., Ivanov, L.M., Kirwan Jr., A.D., Margolina, T.M., 1994. Amount of Cs-137 and Cs-134 radionuclides in the Black sea produced by the Chernobyl disaster. Journal of Environmental Radiology 26, 49–63.

Eremeev, V.N., Ivanov, L.M., Kirwan Jr, A.D., Margolina, T.M., 1995. Analysis of caesium pollution in the Black Sea by regularization method. Marine Pollution Bulletin 30 (7), 460–462.

Hallegraeff, G.M., Jeffrey, S.W., 1985. Description of new chlorophyll a alteration products in marine phytoplankton. Deep-Sea Research 32 (6), 697–705.

Ivanov, L.M., Margolina, T.M., 1996. Reconstruction of oceanographic fields without the information on statistical properties of noise. Proceedings of the Conference of Coastal Oceanic and Atmospheric Prediction. American Meteorological Society, Boston, MA, pp. 155–157.

Ivanov, L.M., Kirwan Jr., A.D., Margolina, T.M., 2001. Filtering noise from oceanographic data with some applications for the Kara and Black seas. Journal of Marine Systems 28 (1–2), 113–139.

Ivanov, L.M., Margolina, T.M., Danilov, A.I., 2004. Application of inverse technique to study radioactive pollution and mixing processes in the Arctic seas. Journal of Marine Systems 48 (1–4), 117–131.

Jeffrey, S.W., Humphrey, G.F., 1975. New spectrophotometric equations for determining chlorophylls *a*, *b*, *c*₁, and *c*₂ in higher plants, algae and natural phytoplankton. Biochemie und Physiologie der Pflanzen 167, 191–194.

Kirk, J.T.O., 1983. Light and photosynthesis in aquatic ecosystems. Cambridge University Press, Cambridge. 401 pp.

Kopelevich, O.V., Sheberstov, S.V., Yunev, O., Basturk, O., Finenko, Z.Z., Nikonov, S., Vedernikov, V.I., 2002. Surface chlorophyll in the Black Sea over 1978–1986 derived from satellite and in situ data. Journal of Marine Systems 36 (3–4), 145–160.

Lofrus, M.E., Carpenter, J.H., 1971. A fluorometric method for determining chlorophyll *a*, *b* and *c*. Journal of Marine Research 29, 319.

Longhurst, A., 1995. Seasonal cycles of pelagic production and consumption. Progress in Oceanography 36, 77–167.

Lorenzen, C.J., Jeffrey, S.W., 1980. Determination of chlorophyll *a* in seawater. SCOR-UNESCO Technical Papers in Marine Sciences, 35, 20 pp.

Mee, L.D., 1992. The Black sea in crisis: a need for concerted international action. Ambio 21 (4), 278–286.

Menke, W., 1984. Geophysical data analysis: discrete inverse theory. Academic Press, New York. 451 pp.

Mikhal'sky, A.I., 1987. Choice of an evaluation algorithm using samples of limited size. Avtomatika i Telemehanika 2, 91–102 (in Russian).

Moberg, L., Robertsson, G., Karlberg, B., 2001. Spectrofluorometric determination of chlorophylls and pheopigments using parallel factor analysis. Talanta 54, 161–170.

Moncheva, S., 2003. On the recent state of the Black Sea ecosystem biological response to eutrophycation—are there signs of recovery uncertainties. In: Preliminary assessment of the previous biogeochemical, hydrophysical, and hydrobiological cruise data within the Black Sea (http://www.blacksea-environment.org/text/ISG/Hydrobiological%20research.pdf), 53 pp.

Morse, P.M., Feshbach, H., 1953. Methods of Theoretical Physics. McGraw-Hill. 997 pp.

Murray, J.W. (Ed.), 1991. Black Sea Oceanography, Results From the 1988 Black Sea Expedition, Deep-Sea Research 38, S665–S1266. Supplementary Issue 2A.

Oguz, T., Salihoglu, B., 2000. Simulation of eddy-driven phytoplankton production in the Black sea. Geophysical Research Letters 27 (14), 2125–2128.

Oguz, T., Latun, V.S., Latif, M.A., Vladimirov, V.V., Sur, H.I., Markov, A.A., Ozsoy, E., Kotovshchikov, B.B., Eremeev, V.V., Ünlüatta, U.U., 1993. Circulation in the surface and intermediate layers of the Black Sea. Deep-Sea Research 40 (8), 1597–1612.

Oguz, T., Ducklow, H., Malanotte-Rizzoli, P., Murray, J.W., Vedernikov, V.I., Unluata, U., 1999. A physical–biological model of plankton productivity and nitrogen cycling in the Black sea. Deep Sea Research: Part 1. Oceanographic Research Papers 46, 597–636.

Oguz, T., Ducklow, H.W., Malanotte-Rizolli, P., 2000. Modeling distinct vertical biogeochemical structure of the Black sea: dynamical coupling of the oxic, suboxic, and anoxic layers. Global Biogeochemical Cycles 14, 1331–1352.

Oguz, T., Malanotte-Rizzoli, P., Ducklow, H.W., Murray, J.W., 2002a. Interdisciplinary studies integrating the Black sea biogeochemistry and circulation dynamics. Oceanography 15 (3), 4–11.

Oguz, T., Deshpande, A.G., Malanotte-Rizzoli, P., 2002b. The role of mesoscale processes controlling biological variability in the Black sea coastal waters: interfences from sea WIFS-derived surface chlorophyll field. Continental Shelf Research 22, 1477–1492.

Oguz, T., Cocacar, T., Malanotte-Rizzoli, P., Ducklow, H.W., 2003. Climatic warming and accompanying changes in the ecological regime of the Black Sea during 1990s. Global Biogeochemical Cycles, 17 (3), 14-1–14-10 (1088).

Ozsoy, E., Unluata, U., 1997. Oceanography of the Black sea: a review of some recent results. Earth-Science Reviews 42, 231–272.

Sabel'feld, K., 1991. Monte-Carlo methods in boundary value problems. Springer-Verlag, Berlin. 274 pp.

Saltzman, B., 1983. Climatic system analysis. Advances in Geophysics 25, 173–233.

Sathyendranath, S., Longhurst, A., Caverhill, C.M., Platt, T., 1995. Regionally and seasonally primary production in the North Atlantic. Deep-Sea Research: Part 1. Oceanographic Research Papers 42 (10), 1773–1802.

Srokosz, M.A., 2000. Biological oceanography by remote sensing. In: Meyers, R.A. (Ed.), Encyclopedia of Analytical Chemistry. John Wiley and Sons Ltd, Chichester, pp. 8506–8533.

Sverdrup, H.U., 1953. On conditions for the vernal blooming of phytoplankton. Journal du Conseil - Conseil Permanent International pour L'exploration de la Mer 18, 287–295.

Thiebaux, H.J., Pedder, M.A., 1987. Spatial Objective Analysis with Applications in Atmospheric Science. Academic Press, New York.

Tikhonov, A.N., Goncharsky, A.V., Stepanov, V.V., Yagola, A.G., 1990. Numerical Methods for Solving Ill-posed Problems. Nauka, Moscow. 223 pp (in Russian).

Trees, C.C., Kennicutt II, M.C., Brooks, J.M., 1985. Errors associated with the standard fluorometric determination of chlorophylls and phaeopigments. Marine Chemistry 17 (1), 1–12.

Vapnik, V.N., Chervonenkis, A.Ya., 1974a. On the method of ordered risk minimization: Part-1. Avtomatika i Telemehanika 8, 21–29 (in Russian).

Vapnik, V.N., Chervonenkis, A.Ya., 1974b. On the method of ordered risk minimization: Part-2. Avtomatika i Telemekhanika 9, 29–39 (in Russian).

Vedernikov, V.I., Demidov, A.B., 1993. Primary production and chlorophyll in deep regions of the Black sea. Oceanology 33, 193–199 (English Translation).

Vedernikov, V.I., Demidov, A.B., 1997. Vertical distribution of primary production and chlorophyll during different seasons in deep regions of the Black sea. Oceanology 37, 376–384 (English Translation).

Yilmaz, A., Tugrul, S., Coban, Y.Y., Yayalta, M., 2001. Nutritional status and primary production in the Black Sea: emphasis on the changes in the last decades, The 5th International Conference on the Environmental Management

of Enclosed Coastal Seas, November 2001, Kobe/Awaji, Japan, EMECS2001 [1–297].

Yunev, O.A., Vedernikov, V.I., Yilmaz, A., 1999. Peculiarity of vertical chlorophyll distribution in the Black and Mediterranean Seas. Proceedings of Joint IAPSO/IABO Symposium "Closed, Semi-closed and Marginal Seas: Physical, Chemical and Biological Properties", Birmingham, England.

Yunev, O.A., Vedernikov, V.I., Basturk, O., Yilmaz, A., Kideys, A.E., Moncheva, S., Konovalov, S., 2002. Long-term variations of surface chlorophyll-*a* and primary production in the open Black sea. Marine Ecology. Progress Series 230, 11–28.

Zaitsev, Yu., Mamaev, V., 1997. Marine Biological Diversity in the Black Sea: A Study of Change and Decline. United Nations Publications. 208 pp.